Available online at www.sciencedirect.com

SciVerse ScienceDirect

Physics Procedia 36 (2012) 1504 – 1509

Physics Procedia

Superconductivity Centennial Conference

Grain structure and irreversibility line of a bronze route CuNb reinforced Nb_3Sn multifilamentary wire

M. J. R. Sandim [a*], D. Stamopoulos [b], E. Aristomenopoulou [b],

S. Zaefferer [c], D. Raabe [c], S. Awaji [d], K. Watanabe [d]a*

[a]Escola de Engenharia de Lorena – USP, 12600-970, Lorena, Brazil
[b]Institute of Materials Science, NCSR "Demokritos", 153-10, Athens, Greece
[c]Max-Planck-Institut für Eisenforshung, D-40237, Düsseldorf, Germany
[d]Institute of Materials Research, Tohoku University, 980-857, Sendai, Japan

Abstract

High-resolution electron backscatter diffraction (EBSD) technique and DC magnetization were used to characterize a Cu-Nb reinforced bronze route Nb_3Sn superconducting multifilamentary wire. The results of DC-magnetization show an extended regime of magnetic reversibility in the operational magnetic field-temperature phase diagram. This observation is discussed in terms of microstructure characteristics of the A15 phase such as grain size, grain boundary misorientation angle distribution, tin gradient across the filaments and residual strain, in connection to the literature.

Keywords: Nb_3Sn; grain structure; irreversibility line; electron backscatter diffraction, DC magnetization

1. Introduction

Nb_3Sn, an intermetallic compound with A-15 type crystal structure, is one of the most important superconducting materials for the generation of high magnetic fields [1-2]. The critical current density in Nb_3Sn depends on the A15 composition, morphology and residual strain [1]. It is well known that for the A-15 phase the grain boundaries are the main flux pinning centers and that the maximum pinning force is inversely proportional to the grain size [1]. Also, to a certain extent, the grain-boundary pinning force

* Corresponding author.
E-mail address: msandim@demar.eel.usp.br

1875-3892 © 2012 Published by Elsevier B.V. Selection and/or peer-review under responsibility of the Guest Editors.
doi:10.1016/j.phpro.2012.06.122

depends on the orientation change across the grain boundary [3]. However, it is still unclear how grain-boundary pinning in Nb_3Sn occurs in detail [1].

Concerning pinning, valuable information can be obtained from the so-called irreversibility line (IL) in the magnetic field-temperature (H-T) phase diagram. This line is the border between the reversible and irreversible regions in the H-T operating phase diagram. Most of the studies concerning the IL are focused on high critical temperature (high-T_c) superconductors [4-5]. However, Suenaga et al. showed that the IL also appears in low-temperature superconducting NbTi and Nb_3Sn multifilamentary wires [6]. They also claimed that the observed IL is a melting line of the flux lattice. After that, the nature of the IL in low-T_c superconductors has been discussed by several authors [7-10].

In this work we performed a study in a bronze route CuNb reinforced Nb_3Sn multifilamentary wire comparing its microstructural and magnetic characteristics. In a previous study the investigated wire was identified as a new and promising candidate for fabrication of react-and-wind coils [2]. Our aim was to examine the possible correlation between the grain structure of the Nb_3Sn phase with the IL exhibited in this multifilamentary wire. The obtained results were compared with relative studies reported in the recent literature, for instance Suenaga et al. [6] and Adesso et al. [11].

2. Experimental

The wire investigated was produced by Furukawa Electric Co. Ltd (Japan) via the bronze method [2]. In this process, a rod of niobium is embedded into a Cu-Sn alloy (bronze) matrix and this arrangement is deformed into a filament form. After multiple repeated bundling, drawing, and restacking operations a multifilamentary wire is obtained. Subsequently the resulting wire is annealed at a suitable temperature (650-700°C or even higher) in order to form the Nb_3Sn phase [2]. This compound is formed as a layer at the interface between Nb and the Sn-rich bronze matrix due to reactive diffusion. As a consequence of the diffusion process there is an inherent Sn gradient in the A15 layer in bronze route filaments. The unreacted Nb core remains surrounded by the A15 phase [2]. The investigated wire (diameter 1 mm) contains 11,457 Nb_3Sn individual filaments in a bronze matrix with composition Cu-14Sn-0.2Ti (in wt.%). This wire was heat treated at 670°C for 96 h. A multifilamentary Cu-21vol%Nb composite is used as reinforcement material in the external part of the wire. It must be noticed that in the as-reacted mode this wire has good superconducting properties with J_c ~ 300 A/mm^2 at 16 T and B_{c2} ~ 23.9 T, at 4.2 K [2], where J_c is the critical current density and B_{c2} is the upper critical magnetic field. The J_c and B_{c2} values can be substantially enhanced by the application of the so-called pre-bent mechanical treatment, which minimizes the residual stress in the wire [2,12]. More details about the design and superconducting properties of this wire can be found in [2]. In this work we report about microstructural and magnetic properties of the Nb_3Sn wire with Cu-Nb reinforcement (CuNb/Nb_3Sn) in the as-reacted mode.

The microstructural characterization of the Cu-Nb/Nb_3Sn wire was performed using high resolution Electron Backscatter Diffraction (EBSD) technique. For the EBSD maps, the cross-section of the investigated wire was Ar-ion polished using the precision etching coating system GATAN – Model 682. EBSD data from four Nb_3Sn filaments were determined by means of automated acquisition and further indexing of Kikuchi patterns after suitable image processing in a TSL EBSD system interfaced to a JEOL JSM-6500F field emission scanning electron microscope (FEG-SEM). DC magnetization measurements were performed using a Superconducting Quantum Interference Device (SQUID) magnetometer (Quantum Design), with a magnetic field applied perpendicular to the wire axis. Isofield magnetization curves, m(T), were obtained in both the zero-field cooled (ZFC) and field cooled (FC) conditions in the temperature range $4<T<20$ K, for several values of the DC magnetic field up to 50 kOe.

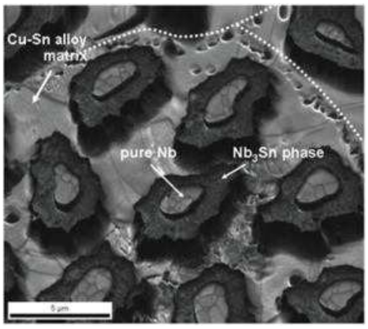

Fig. 1. SEM image of Nb_3Sn filaments in the cross-section of the investigated wire.

3. Results and discussion

Figure 1 shows a cross sectional view of the Nb_3Sn filaments in the wire. The unreacted polycrystalline Nb core is clearly visible. The A15 layer has a typical thickness of about 1.5 μm. Kirkendall pores can also be observed in the Cu-Sn bronze matrix (see white dotted track curves). A detailed view of a typical Nb_3Sn filament is shown in Fig. 2(a). The corresponding grain boundary map related to A15 phase is shown in Fig. 2(b). In this figure black (majority population) and red (minority population) lines correspond to high ($\psi > 15^o$) and low ($\psi < 15^o$) angle boundaries, respectively, where ψ is the misorientation angle that quantifies the difference in the crystallographic orientations between two crystallites in a polycrystalline material. The cross-section observation shows equiaxed and elongated grains coexisting in the microstructure of the Nb_3Sn phase. The average grain size is about 135±70 nm. At first sight, Fig. 2(b) suggests that small areas of Nb_3Sn phase are also found along grain boundaries within the Nb core. However, these areas are most probably due to false indexing of low–quality diffraction patterns in areas close to Nb grain boundaries, as discussed elsewhere [13].

Figure 3 shows the correlated misorientation angle distribution, normalized to unit, as measured across the boundaries in the Nb_3Sn phase for the filament shown in Fig. 2. An important characteristic of such a distribution is the presence of a large fraction of high-angle boundaries. The peak observed for low-angle grain boundaries (2-5^o) in the microstructure in part is due to the orientation scatter in the EBSD data in the Nb_3Sn phase and, therefore, must be disregarded [13]. Furthermore, the misorientation angle distribution shown in Fig. 3 resembles the Mackenzie distribution [14], indicated by a red line for reference. The Mackenzie distribution describes the grain boundary misorientation angle distribution in a randomly oriented set of grains with cubic symmetry [14]. According to Togano, a random distribution of orientations with a large fraction of high-angle boundaries is essential to improve pinning of flux lines at the grain boundaries, i.e., the larger the misorientation at an interface is, the larger the pinning force at that boundary [3]. From this point of view, it is expected that the investigated CuNb/Nb_3Sn wire presents excellent shielding properties. However, in terms of improving pinning a general assumption for the Nb_3Sn phase is that the optimum grain size must be less than 100 nm [1], what is not the case for the investigated CuNb/Nb_3Sn wire.

For analyzing further the pinning characteristics of the investigated Nb_3Sn multifilamentary wire, we performed DC magnetization measurements for both ZFC and FC protocols for several applied fields in the range 1 kOe < H < 50 kOe. Representative DC magnetization curves are displayed in Fig. 4. From these data we have identified a temperature range below the critical temperature, T_c, where the flux motion is reversible.

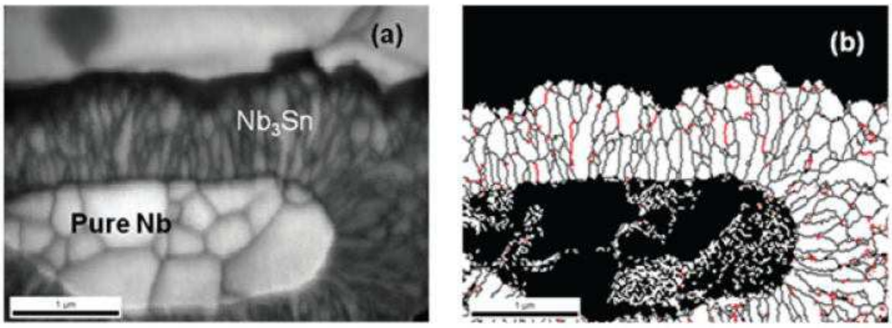

Fig. 2. (a) EBSD image quality map of a typical Nb_3Sn filament; (b) the corresponding boundary map of the Nb_3Sn phase. High- and low-angle boundaries are displayed by black and red lines, respectively.

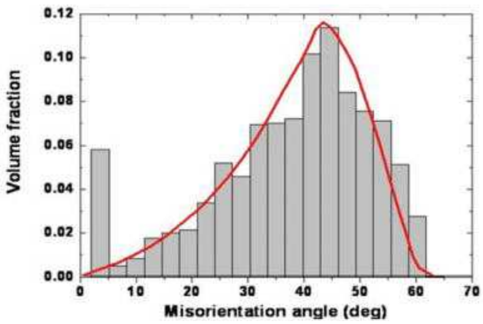

Fig. 3. Misorientation angle distribution, normalized to unit, as measured across boundaries in the Nb_3Sn phase for the filament shown in Fig. 2. The Mackenzie distribution [14] is included (in red) for comparison.

The magnetic-field dependence of the lower boundary of this temperature region is the so-called irreversibility temperature, $T_{ir}(H)$. Figure 4(d) illustrates, for H = 50 kOe, the criteria which were used for determining the irreversibility temperature $T_{ir}(H)$ as well as the critical temperature $T_c(H)$.

The obtained $T_{ir}(H)$ and $T_c(H)$ curves are summarized in the H-T phase diagram displayed in Figure 5 together with the respective curves reported by Suenaga et al. [6] for other Nb_3Sn multifilamentary wire. It is important to stress that these curves were obtained from DC magnetic measurements, using the same criterion. In our data set the IL can be clearly distinguished from the upper-critical field line, B_{c2}, in agreement with the results reported in [6]. However, we see that the CuNb/Nb_3Sn wire investigated in this work exhibits an extended regime of reversible behavior when contrasted to the data reported by Suenaga et al. [6]. For example, at 3 T the temperature range of reversible flux motion for the CuNb/Nb_3Sn wire studied here is significantly larger (~ 1.5 K) than that (~ 0.9 K) reported in Ref. [6]. A similar observation can be done when we compare the H-T phase diagram for the investigated wire with those obtained for Adesso et al. [11] for another bronze route multifilamentary wire, although in Ref. [11] the field-temperature phase diagram was obtained from AC magnetic measurements. According to Ref. [11] the Sn gradient contributes to the separation between IL and B_{c2} lines. For the bronze route multifilamentary wire reported in Ref. [11] it was observed a tin gradient from 17 to 25at%. According to Ref. [15] such tin gradient corresponds to a T_c distribution from approximately 10 to 18 K. Concerning T_c distribution of the Nb_3Sn wire investigated in the present work, the transition width concerning the Nb_3Sn phase is $\sim$ 2.3 K [2], lower than the correspondent one for the bronze route Nb_3Sn wire reported in Ref. [11].

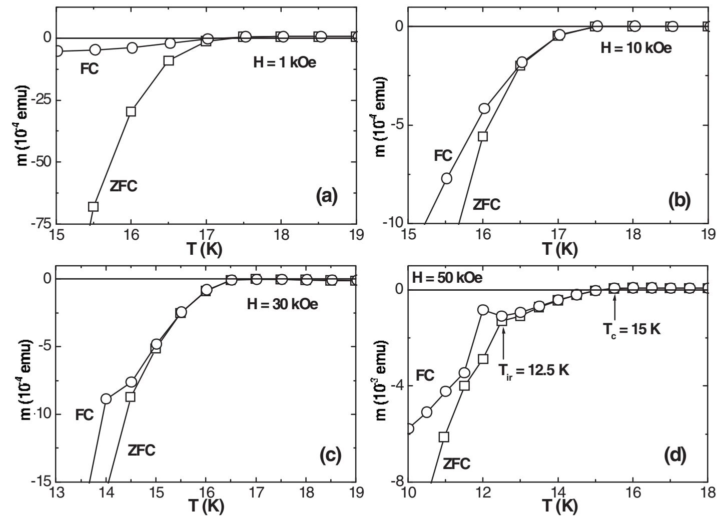

Fig. 4. m(T) curves (ZFC and FC conditions) for the Nb_3Sn wire, for field applied perpendicular to the wire axis using (a) H = 1 kOe, (b) H = 10 kOe, (c) H = 30 kOe and (d) H = 50 kOe, which shows the criteria used for determination of both T_c and T_{ir}.

Unfortunately, data concerning the average grain size for the Nb_3Sn wire reported in Ref. [11] are not available for comparison, as well as data concerning the grain structure for the Nb_3Sn wire reported by Suenaga et al in Ref. [6]. Therefore, in spite of its optimum grain boundary misorientation angle distribution, the CuNb/Nb_3Sn wire investigated in the present work exhibits an extended reversibility regime, when compared with results reported in literature [6,11]. Such behavior can be attributed to the relatively large mean grain size of the Nb_3Sn phase and to the Sn gradient. Furthermore, an important difference between the Nb_3Sn wire investigated in this work and those reported in Ref. [6,11] is the presence of CuNb reinforcement in the external part of the former conductor. Such reinforcement can establish intense residual strain to the CuNb/Nb_3Sn wire that can be another factor contributing to the large difference between IL and B_{c2} lines observed in this work.

4. Conclusions

In summary, for a bronze route Cu-Nb reinforced Nb_3Sn multifilamentary wire with high values of J_c and B_{c2}, we observed that the Nb_3Sn phase is characterized by a random distribution of grain boundaries orientations with a large fraction of high-angle boundaries. The average grain size of the Nb_3Sn phase is about 135 ± 70 nm. In spite of the optimum grain boundary misorientation angle distribution for improving pinning, this wire presents a clearly distinguished irreversibility line in the H-T phase diagram, with an extended regime of reversible behavior. Such behavior can be attributed to microstructure characteristics of the A15 phase that is the relatively large grain size, the tin gradient across the filaments and possibly to the residual strain.

Acknowledgements

This work was partially supported by the Brazilian Financial Agency FAPESP (Grant 06/61753-2).

M. J. R. Sandim is grateful also to CAPES-DAAD (Grant A/08/01572) and to CNPq (Brazil) for the financial support. Thanks are also due to Furukawa Electric Co. Ltd (Japan) for supplying the Nb_3Sn wires for this investigation.

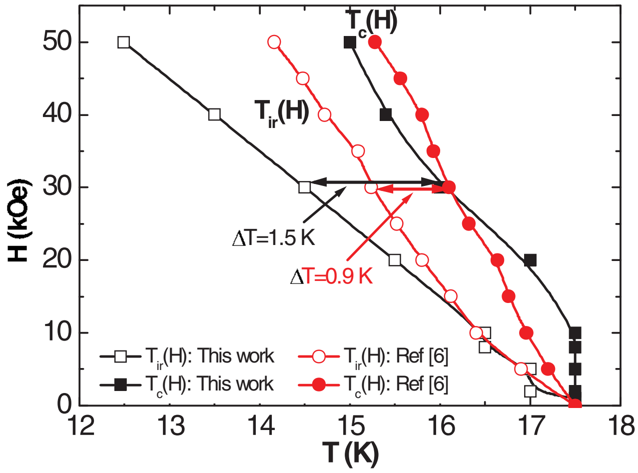

Fig. 5. H-T phase diagram for the investigated Nb_3Sn wire, obtained from the m(T) curves. The correspondent data reported by Suenaga et al. in Ref. [6] are also displayed for comparison.

References

[1] Godeke A. A review of the properties of Nb_3Sn and their variation with A15 composition, morphology and strain state. *Supercond Sci Technol*. 2006; **19:** R68 – R80.

[2] Badica P, Awaji S, Nishijima G, Oguro H, Sandim MJR, Cangani MP, et al. Performance of as-reacted and multiple bent ("pre-bent") practical Nb_3Sn bronze route wires with different architectures. *Supercond Sci Technol* 2007; **20:** 273-280.

[3] Togano K, Tachikawa K. Textures in diffusion-porcessed superconducting Nb_3Sn and V_3Ga layers. *J Appl Phys* 1979;**50:** 3495-3499.

[4] Gupta A, Esquinazi P, Braun HF, Neumüller HW. Thermally activated depinning in polycrystalline Bi-based high-T_c superconductors. *Phys Rev Lett* 1989;**63**: 1869-1872.

[5] Stamopoulos D, Pissas M, Bondarenko A. Possible reordering of vortex matter near the end point of the second peak line in the $YBa_2Cu_3O_{7-\delta}$ compound. *Phys Rev B* 2002;**66**: 214521-2145217.

[6] Suenaga M, Ghosh AK, Xu Y, Welch DO. Irreversibility temperatures of Nb_3Sn and Nb-Ti. *Phys Rev Lett* 1991;**66**: 1777 - 1780.

[7] Watanabe K. On the irreversibility line in superconductors. *Jpn J Appl Phys*1992;**31**: L1586 – L1588.

[8] Schmidt MF, Israeloff NE, Goldman AM. Applicability of high-T_c paradigms to magnetic relaxation and irreversibility in superconducting Nb. *Phy. Rev B* 1993;**48**: 3404-3416.

[9] Zheng DN, Ingle NJC, Campbell AM. Irreversibility fields of superconducting niobium alloys. *Phys Rev B* 2000;**61**: 15429-15435.

[10] Stamopoulos D, Speliotis A, Niarchos D. From the second magnetization peak to peak effect. A study of superconducting properties in Nb films and MgB_2 bulk samples. *Supercond Sci Technol* 2004;**17**: 1261-1274.

[11] Adesso MG, Flukiger R, Uglietti D, Polichetti M, Pace S. Influence of grain boundaries and Sn distribution on the H-T phase diagram of Nb_3Sn. *IEEE Trans Appl Supercond* 2007;**17**: 2619- 2622.

[12] Awaji S, Watanabe K, Katagiri K. Improvement of mechanical and superconducting properties in CuNb/(Nb, $Ti)_3Sn$ wires by applying bending strain at room temperature. *Supercond Sci Technol* 2003;**16**: 733-738.

[13] Sandim MJR, Sandim HRZ, Zaefferer S, Raabe D, Awaji S, Watanabe K. Electron backscatter diffraction study of Nb_3Sn superconducting multifilamentary wire. *Scripta Mater* 2010; **62**: 59-62.

[14] Mackenzie JK. The distribution of rotation axes in a random aggregate of cubic crystals. *Acta Metall* 1964; **12**: 223-225.

[15] Wang Y, Senatore C, Abächerli V, Uglietti D, Flükiger R. Specific heat of Nb_3Sn wires. *Supercond. Sci. Technol*. 2006;**19**: 263-266.